Ann. Geophys., 28, 1499–1509, 2010
www.ann-geophys.net/28/1499/2010/
doi:10.5194/angeo-28-1499-2010

Annales Geophysicae

Intermediate-*m* ULF waves generated by substorm injection: a case study

T. K. Yeoman[1], **D. Yu. Klimushkin**[2], **and P. N. Mager**[2]

[1]Department of Physics and Astronomy, University of Leicester, Leicester LE1 7RH, UK
[2]Institute of Solar-Terrestrial Physics, Irkutsk, P.O. Box 291, 664033, Russia

Received: 26 May 2010 – Accepted: 2 August 2010 – Published: 5 August 2010

Abstract. A case study of SuperDARN observations of Pc5 Alfvén ULF wave activity generated in the immediate aftermath of a modest-intensity substorm expansion phase onset is presented. Observations from the Hankasalmi radar reveal that the wave had a period of 580 s and was characterized by an intermediate azimuthal wave number (m=13), with an eastwards phase propagation. It had a significant poloidal component and a rapid equatorward phase propagation ($\sim$62° per degree of latitude). The total equatorward phase variation over the wave signatures visible in the radar field-of-view exceeded the 180° associated with field line resonances. The wave activity is interpreted as being stimulated by recently-injected energetic particles. Specifically the wave is thought to arise from an eastward drifting cloud of energetic electrons in a similar fashion to recent theoretical suggestions (Mager and Klimushkin, 2008; Zolotukhina et al., 2008; Mager et al., 2009). The azimuthal wave number m is determined by the wave eigenfrequency and the drift velocity of the source particle population. To create such an intermediate-m wave, the injected particles must have rather high energies for a given L-shell, in comparison to previous observations of wave events with equatorward polarization. The wave period is somewhat longer than previous observations of equatorward-propagating events. This may well be a consequence of the wave occurring very shortly after the substorm expansion, on stretched near-midnight field lines characterised by longer eigenfrequencies than those involved in previous observations.

Keywords. Ionosphere (Wave-particle interactions) – Magnetospheric physics (Magnetosphere-ionosphere interactions; MHD waves and instabilities)

Correspondence to: T. K. Yeoman
(tim.yeoman@ion.le.ac.uk)

1 Introduction

Magnetospheric long-period Ultra Low Frequency (ULF) waves in the Pc 3–5 frequency band (2–100 mHz) in the terrestrial magnetosphere represent Alfvén waves standing between magnetically conjugate points of the high-conductivity ionosphere. These waves are usually categorized according to their predominant polarization: toroidal waves if the perturbed magnetic field oscillates in an azimuthal direction, and poloidal waves if the magnetic field oscillates in a radial (meridional) direction. Furthermore, these two kinds of waves are distinguished according to their azimuthal wave number m: the toroidal modes are generally low-m waves (or equivalently a large scale size in the azimuthal direction) and the poloidal modes are high-m waves (or equivalently a small scale size in the azimuthal direction). The two wave modes are thought to have distinct generation mechanisms. The low-m waves are usually supposed to be resonantly generated by an incoming fast mode arriving from the outer boundary of the magnetosphere (field line resonance) (e.g., Agapitov et al., 2009). The high-m waves generally have $m > 15$, and are thought to have their energy source in drifting energetic particle fluxes entering the Earth's inner magnetosphere from the magnetotail and subsequently experiencing gradient-curvature drift and thus moving around the Earth, constituting part of the global ring current (e.g., Baddeley et al., 2005b,a). These energetic particles can drive MHD wave modes through wave-particle interactions, for example via the drift and drift-bounce resonance interactions, leading to perturbations in the electric and magnetic fields in the magnetosphere and ionosphere when free energy is available to the wave. Such high-m waves are presently a topic of considerable importance in both theoretical and experimental studies. In much previous work it has been suggested (e.g., Southwood, 1976; Hughes et al., 1978, 1979) that the part of

the ion distribution function which is able to feed energy into the wave is that where

$$\partial f \big/ \partial W > 0, \tag{1}$$

where f is the ion distribution function and W is the energy. Such non-Maxwellian ion distribution functions, often termed "bump-on-tail" distributions, can be created quite commonly by naturally-occurring processes in the magnetosphere, such as substorm-associated particle injections or other particle acceleration processes. Subsequent to such an injection the ions are subject to gradient-curvature and $\boldsymbol{E} \wedge \boldsymbol{B}$ drifts and move westwards, arriving at a given magnetic local time at different universal times due to the energy dependence of magnetospheric drift paths. Even under steady state conditions particles follow energy-dependent drift paths which can lead to the formation of such bump-on-tail distributions (Cowley and Ashour-Abdallah, 1976; Glassmeier et al., 1999a; Ozeke and Mann, 2001). Subsequent to such an injection and drift process, on occasion particles will match the local drift-bounce resonance condition (Southwood et al., 1969),

$$\omega_{\text{wave}} - m_{\text{wave}}\omega_{\text{d}} = N\omega_{\text{b}}, \tag{2}$$

where N is either zero (drift resonance) or an integer (usually ± 1, drift bounce resonance). In either case ω_{wave}, ω_{b}, and ω_{d} are the angular frequencies of the wave, the proton bounce, and the proton azimuthal drift, respectively. Such wave-particle interactions are processes of fundamental importance in collisionless astrophysical plasmas.

Although this picture seems generally accepted, there are some inconsistencies concerning the generation of the low-m waves. Some key features of field line resonances have yet to be observed (Glassmeier et al., 1999b). In addition, due to the very different spatial structure of the Alfvén and fast modes their interaction is rather weak and the generation mechanism may become rather ineffective (Leonovich, 2001). Saka et al. (1992) also observed a Pc5 wave event with $m \sim 1$ associated with increased fluxes of energetic electrons in the magnetosphere and interpreted it as a wave generated not through coupling between a fast and Alfvén mode, but rather by electron injection. These facts hint that some low- and intermediate-m waves can be generated through mechanisms other than resonant excitation by the fast mode, perhaps by high energy particles, as suggested for the high-m wave populations.

In previous work the structure and occurrence of energetic particle-driven waves have been studied by a number of authors in the magnetosphere with in situ spacecraft data, for both case studies (e.g., Hughes et al., 1979; Takahashi et al., 1990; Eriksson et al., 2006; Schäfer et al., 2007, 2008) and statistically (e.g., Kokubun, 1985; Takahashi et al., 1985; Anderson et al., 1990; Woch et al., 1990; Engebretson et al., 1992; Lessard et al., 1999). These studies identified a strong population of particle-driven waves in the dusk sector. Events were also detected near dawn, however, and a variety of wave-particle interaction modes have been invoked. Ground-based observations have also contributed greatly to our knowledge of particle-driven waves. A number of categories of waves have been identified in such data, which have distinct wave characteristics and occurrence conditions. Giant "Pg" pulsations have been observed on the ground and in situ by orbiting satellites at times when geomagnetic conditions are quiet. A statistical study of 34 of these events observed on the EISCAT magnetometer cross network in northern Scandinavia found a peak in occurrence of these waves in the dawn/prenoon sector; no events were observed in the afternoon (Chisham and Orr, 1991). The average value of the azimuthal wave number was ~ -26 for the 34 events (here negative m is taken to represent westward phase propagation). Pgs have been related to drift-bounce resonance mechanisms with both symmetric (e.g., Takahashi et al., 1992) and antisymmetric (e.g., Chisham and Orr, 1991) wave modes, and the wave-particle interaction responsible for their generation thus remains controversial.

Storm time Pc5 pulsations have been seen in STARE (the Scandinavian Twin Auroral Radar Experiment; Greenwald et al., 1978) data (Allan et al., 1982, 1983). Storm time Pc5 pulsations are compressional waves of high m number ($m = -20$ to -80) with a frequency in the Pc5 range (1.7–6.7 mHz) which have been associated with a drift-resonance source mechanism. Drift resonance involves fundamental wave modes, with the electric field symmetric about the equator (i.e. an equatorial electric field antinode). Contrary to the Pg events discussed above, storm-time Pc5s are observed in the dusk sector during magnetically disturbed intervals.

Some more recent results from a High Frequency (HF) Doppler sounder, DOPE (the DOppler Pulsation Experiment; Wright et al., 1997) at Tromsø, northern Norway have demonstrated the existence of populations of high-m waves in both the morning and afternoon sectors. In this case the morning sector waves were the most populous, and had m-numbers of order 100, high enough to screen the waves completely from ground magnetometers (Yeoman et al., 2000). In later studies using DOPE, Baddeley et al. (2005a) demonstrated that waves with m-numbers of 100–200 were associated with a source in proton populations with energies $\sim$10 keV, with a drift-bounce resonance mechanism most likely in the prenoon sector, but with both drift- and drift-bounce resonance mechanisms possible in the postnoon sector. Using a combination of DOPE observations and in situ energetic particle measurements, Baddeley et al. (2005b) were able to demonstrate a statistically significant relationship between such high-m wave occurrence and conjugate measurements of non-Maxwellian particle populations in the overlying magnetosphere.

Another classification of high-m waves, similar to those described above, but with an equatorward phase motion, have been seen in SABRE (the Sweden And Britain auroral Radar

Experiment; Nielsen et al., 1983) coherent radar system in the dusk sector (Waldock et al., 1983; Tian et al., 1991; Yeoman et al., 1992). Similar observations were seen in the BARS (Bistatic Auroral Radar System; McNamara et al., 1983) coherent radar by Grant et al. (1992). Later, Yeoman and Wright (2001) presented ULF wave observations close to local noon using the HF radar artificial backscatter technique at Tromsø which demonstrated both wave activity characteristic of drift-bounce resonance and wave activity characteristic of drift resonance activity, with the latter waves showing equatorward phase propagation. Recently Yeoman et al. (2008) presented observations of similar populations of equatorward-propagating wave events driven by energetic particle populations in the outer magnetosphere, at an L-shell of 15. These previous observations of equatorward propagating waves are the most similar observations to a newly identified population of ULF wave events, where an equatorward propagating wave which is characterised by an intermediate azimuthal wave number is associated with a newly-injected energetic particle population. An exemplary case study of such a wave is presented here, and its possible source mechanism is discussed.

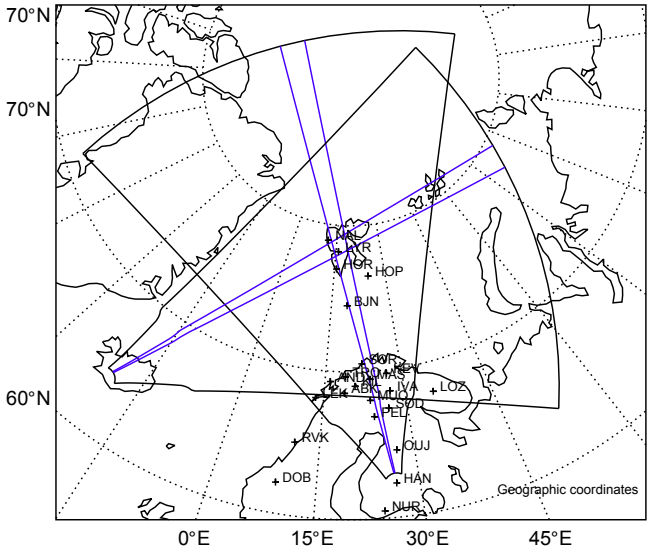

Fig. 1. The fields of view of Channel A (black) and Channel B (blue) of the Hankasalmi, Finland and Þykkvibær, Iceland SuperDARN radars during the interval under study.

2 Instrumentation

The ULF wave data presented here were recorded by the SuperDARN radars at Hankasalmi, Finland and Þykkvibær, Iceland. Full details of SuperDARN are given in Greenwald et al. (1995) and Chisham et al. (2007). Figure 1 presents the fields of view of the radar scan modes used in this study. Channel A of both radars employed a full 16-beam scan of 45 km range gates, starting at a range of 180 km, and is outlined in black. Channel B was restricted to 1 beam, again with 45 km range gates. Hankasalmi sounded beam 9, pointing northwards, whereas Þykkvibær sounded beam 5, pointing north and east. These beams are outlined in blue in Fig. 1. The integration time of the radars was 3 s, yielding a full radar scan from Channel A every minute, and single beam data with 3 s time resolution on Channel B. Data are also presented from the IMAGE (International Monitor for Auroral Geomagnetic Effects; Lühr, 1994) magnetometer array, which has a sampling interval of 10 s. The time intervals under study were selected from intervals identified using the FUV instrument (Mende et al., 2000a,b) on the IMAGE spacecraft. Specifically use is made of the list of 2437 substorm events occurring between May 2000 and December 2002 identified by Frey et al. (2004). This list was subsequently extended to 4193 substorm events after considering the 5-year period up to December 2005.

3 Data

The ULF wave event case study presented here occurred on 21 March 2002, and was selected from a dataset derived from the IMAGE substorm list described in Sect. 2. The list of substorm events was reduced by selecting substorm onset events which occurred within 1 h local time of the location of the Hankasalmi radar. The list was further reduced by selecting only those times when a high time resolution beam was available on beam 9 of the Hankasalmi radar, and good quality data coverage was available on both the Hankasalmi and Þykkvibær radars. The data coverage and substorm development are indicated in Fig. 2. The upper panels of Fig. 2 present the data coverage of the two SuperDARN radars, showing the colour-coded ionospheric flow velocities across the full fields of view at 23:37 UT. The Hankasalmi data are presented in Fig. 2a and the Þykkvibær data in Fig. 2b. Red (negative) velocities are away from the radar and blue (positive) velocities are towards the radar. The data are presented in magnetic latitude-magnetic local time coordinates. The radial dashed lines are separated by 1 h local time, with local midnight being marked by the vertical dashed line. The dashed circles indicate magnetic latitude at 10° separations. Excellent data coverage is seen across a substantial region of both radar fields-of-view. The lower panels Fig. 2c–e present the corresponding IMAGE FUV Wideband Imaging Camera (WIC) instrument in the same coordinate system. The substorm onset was identified by Frey et al. (2004) as starting at 23:35:19 UT, at a geomagnetic latitude of 66.76° and a magnetic local time of 02:00. Fig. 2c shows the auroral signature of the substorm at the identified onset time. Note that the substorm onset, although clear, was of modest intensity. The peak IMAGE WIC intensity was relatively weak, the AE index at onset was 88 nT, peaking at 135 nT 1 h after onset, and no significant particle injection activity was observed by the LANL geostationary spacecraft on field lines

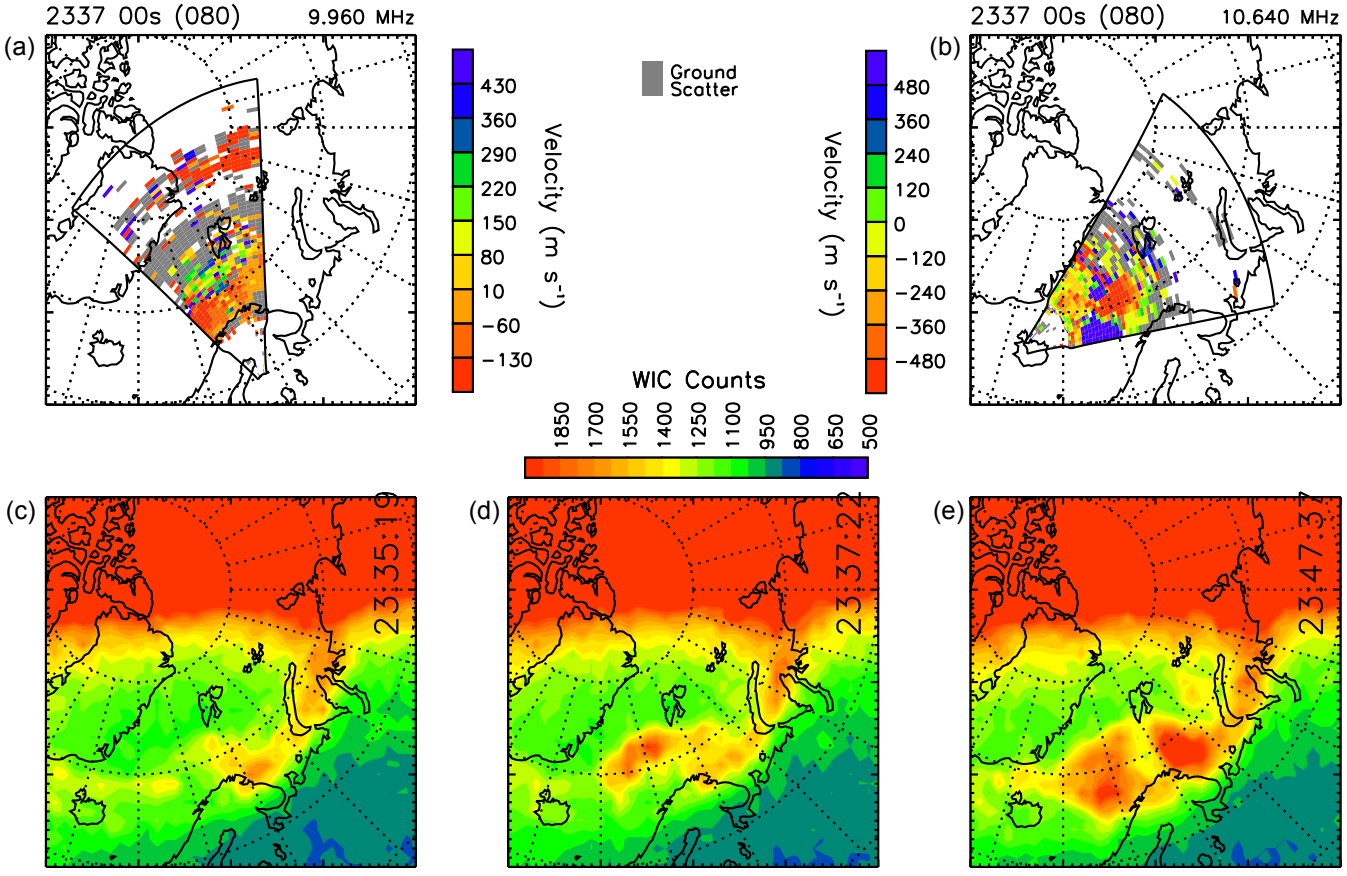

Fig. 2. Fields-of-view and data coverage from Channel A of the SuperDARN radars at **(a)** Hankasalmi, Finland and **(b)** Þykkvibær, Iceland in magnetic latitude-magnetic local time coordinates during substorm onset at 23:37 UT. Red (negative) velocities are away from the radar and blue (positive) velocities are towards the radar. The radial dashed lines are separated by 1 h local time, with local midnight being marked by the vertical dashed line. The dashed circles indicate magnetic latitude at 10° separations. **(c–e)** present IMAGE WIC auroral data in the same coordinate system for three times during the substorm expansion phase.

equatorward of the observations presented here. Figure 2d and e shows the subsequent development of the auroral emissions at 23:37:22 UT and 23:47:37 UT. By 23:37:22 UT the auroral activity had migrated poleward and westward over the westernmost limit of the SuperDARN radar data coverage, and subsequently by 23:47:37 UT the auroral activity expanded in all directions, essentially filling the area of the SuperDARN radar data.

Figure 3 presents IMAGE X-component magnetometer data during the substorm interval. Figure 3a depicts unfiltered data between 22:00 UT and 02:00 UT for a selection of IMAGE stations covering decreasing latitudes from top to bottom. At the highest and lowest stations there is little magnetic signature of the substorm activity, but between these stations there is a clear decrease in the X component magnetic field, starting around 23:30 UT, indicating an enhanced westward electrojet associated with the substorm. Figure 3b presents the same data, but now bandpass filtered between 1000–20 s for the interval 23:30–00:30 UT. Here the ground magnetometer data provide evidence for some ULF wave activity occurring in the hour following the substorm onset, with a period in the region of 600 s. SuperDARN radar measurements of this ULF wave activity as measured directly in the ionospheric flow velocities is presented in Fig. 4. The data from Hankasalmi beam 9 is presented in Fig. 4a and the data from Þykkvibær beam 5 is presented in Fig. 4b. The ionospheric velocities are colour-coded as in Fig. 2, and the location of these two high time resolution beams is illustrated in Fig. 1. The wave activity suggested by the IMAGE magnetometer data in Fig. 3b is clearly visible in the ionospheric flow velocity from both radars. The meridional beam of the Hankasalmi radar presented in Fig. 4a reveals

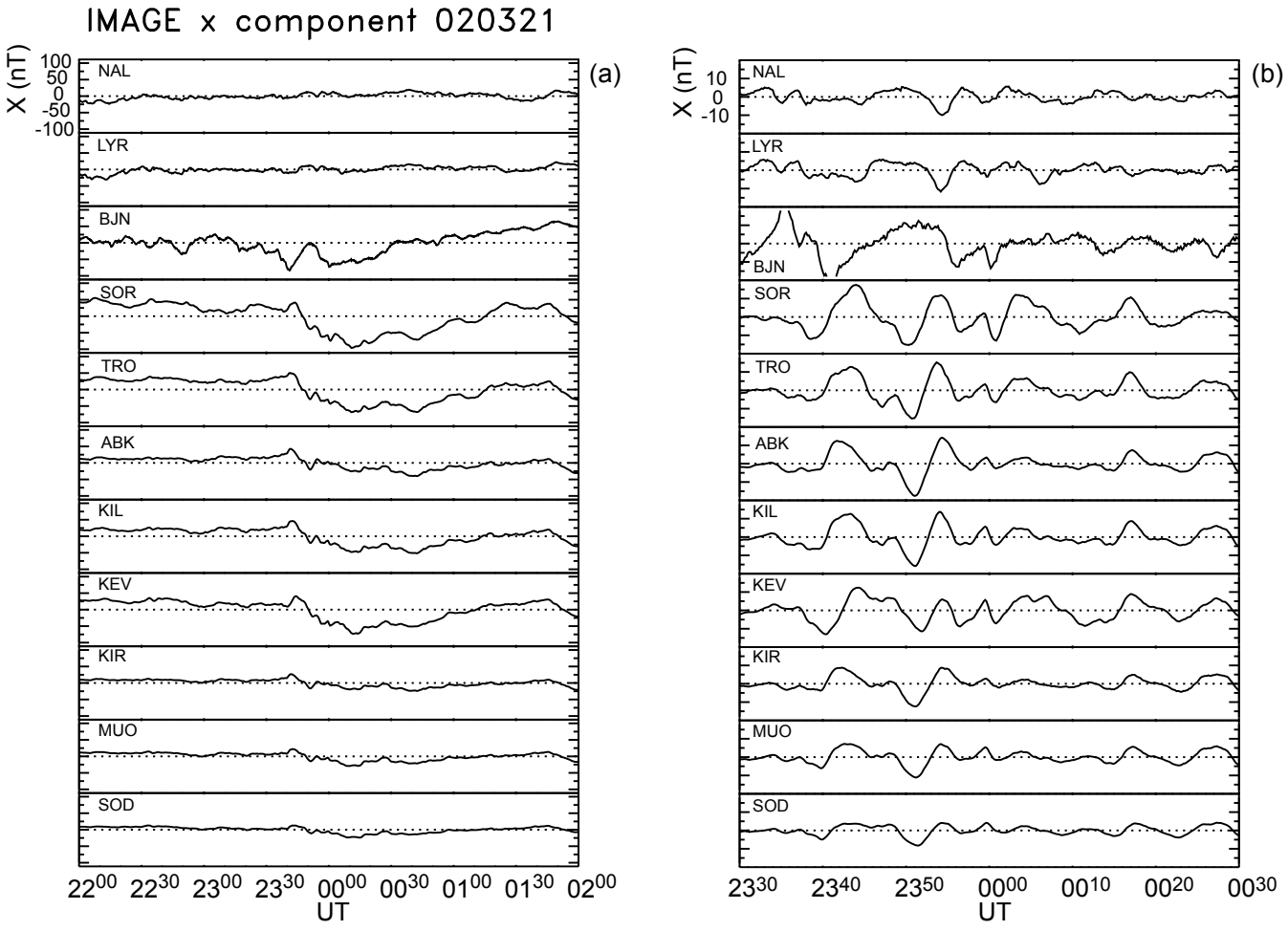

Fig. 3. IMAGE X-component magnetometer data during the substorm interval. **(a)** unfiltered data between 22:00 UT and 02:00 UT **(b)** data bandpass filtered between 1000–20 s for the interval 23:30–00:30 UT.

oscillatory flow velocities covering magnetic latitudes of 66° to 76°, with a clear equatorward phase evolution visible in the wave. Fourier analysis (not shown) reveals the wave period to be 580 s (a frequency of 1.7 mHz). The data from the north-east directed beam of the Þykkvibær radar in Fig. 4b shows wave activity with the same period, but with little detectable phase propagation in the direction of the radar beam.

The Fourier amplitude and phase behaviour of the wave is now examined in more detail. Figure 5a and b present the Fourier power and phase at the peak frequency of the ULF wave as a function of geomagnetic latitude, as derived from the ionospheric drift velocity measurements along beam 9 of the Hankasalmi SuperDARN radar presented in Fig. 4a. A 3° latitude range is chosen, where the wave signatures are clearest and free from ground scatter contamination. The Fourier analysis confirms the equatorward phase propagation, revealing that the wave exhibits a phase propagation of 151° over this latitude range ($\sim 62°$ per degree of latitude). It is visually clear from Fig. 4a that the total equatorward phase variation over the wave signatures visible in the radar field-of-view exceed the 180° associated with field line resonances. Figure 6 similarly presents Fourier (a) power and (b) phase at the peak frequency of the ULF wave observed in the ionospheric drift velocity, but now as measured along beams 7–12 of the Hankasalmi SuperDARN radar at 70° magnetic latitude, as a function of geomagnetic longitude. This required using the lower time resolution (1 min) beams of the Hankasalmi radar, in which the wave activity is not so well resolved, but the data are adequate for Fourier analysis of the 580 s wave. An eastward phase propagation of 116° is observed over this longitude range (corresponding to an effective azimuthal wave number m of ~ 13). Finally Fig. 7 presents Fourier (a) power and (b) phase at the peak frequency of the ULF wave observed in the ionospheric drift velocity measured along beam 5 of the Þykkvibær SuperDARN radar as a function of geomagnetic longitude (the corresponding geomagnetic latitudes of the datapoints are shown on the right for reference). Here only a small total phase propagation is apparent (a 13° decrease), with the phase seeming to decrease with magnetic longitude in the west and increase in the

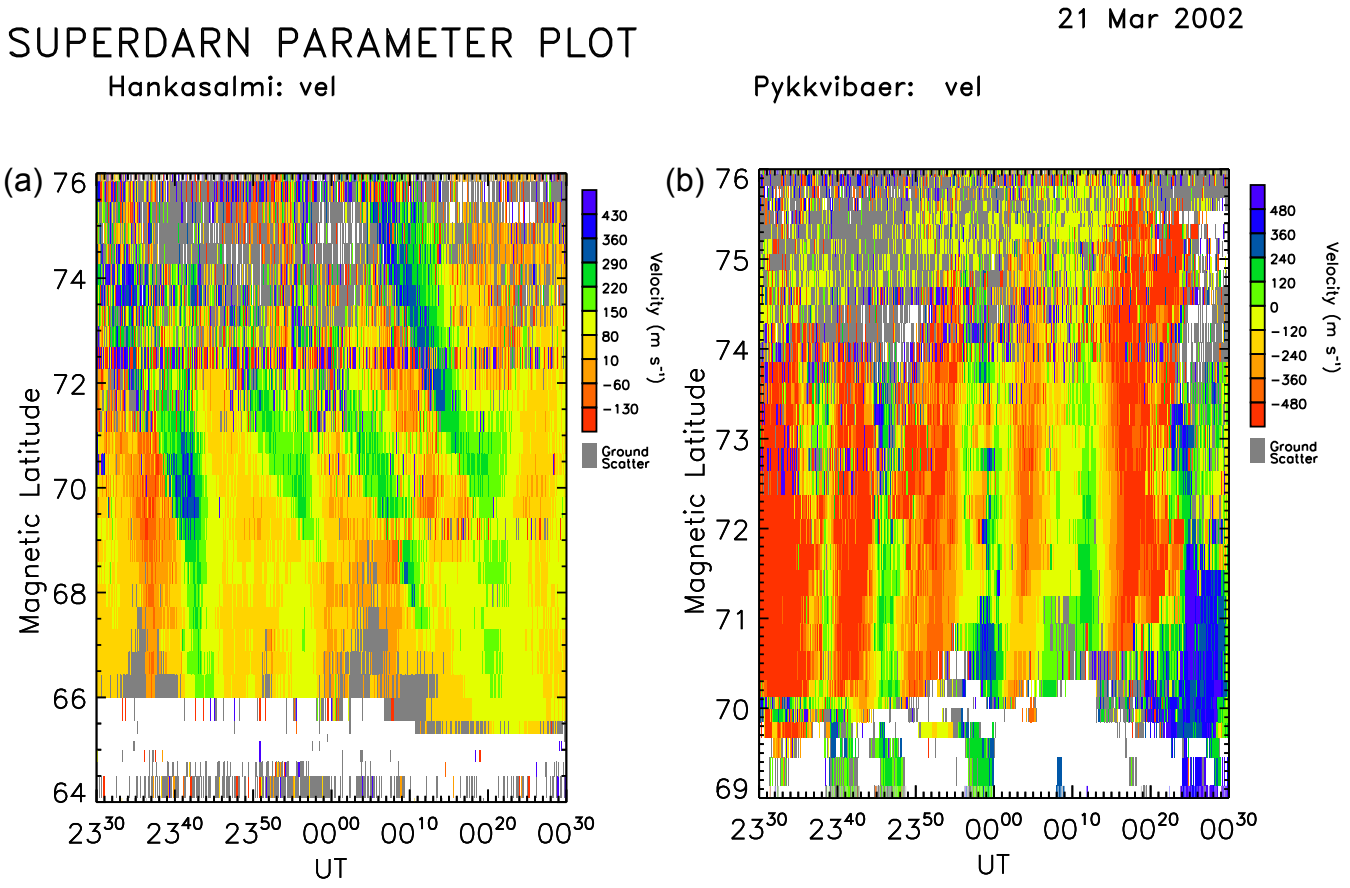

Fig. 4. SuperDARN radar velocity measurements from **(a)** Hankasalmi beam 9 and **(b)** Þykkvibær beam 5. The ionospheric velocities are colour-coded as in Fig. 2, and the location of these two high time resolution beams is illustrated in Fig. 1.

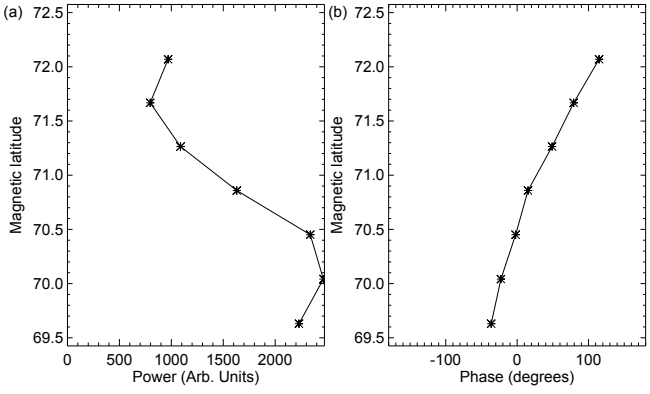

Fig. 5. Fourier **(a)** power and **(b)** phase at the peak frequency of the ULF wave observed in the ionospheric drift velocity measured along beam 9 of the Hankasalmi SuperDARN radar as a function of geomagnetic latitude.

east, although the significance of such small phase variations is unclear. If the longitudinal and latitudinal phase propagations observed in the Hankasalmi data are used to predict the phase evolution expected along Þykkvibær beam 5, which covers a significant range of both latitude and longitude, then a phase increase of 103° in latitude and a phase decrease of 80° in longitude result. Thus the small phase change observed along Þykkvibær beam 5 is essentially consistent with the data from the Hankasalmi radar.

4 Interpretation: Alfvén waves, generated by substorm injected high-energy particles

The ULF wave activity considered in the previous section shows a number of characteristic features. The wave is characterised by an intermediate azimuthal wave number. It has a significant poloidal component and a rapid equatorward phase propagation. It is also observed in the immediate aftermath of a substorm expansion phase onset, collocated with the substorm auroral expansion, and thus we assume closely associated with the substorm energetic particle injection. As such the wave activity is most similar to previous observations of equatorward propagating ULF waves. Previous observations of such events have suggested that they are predominantly observed in the dusk sector, and they have been associated with westward drifting proton populations

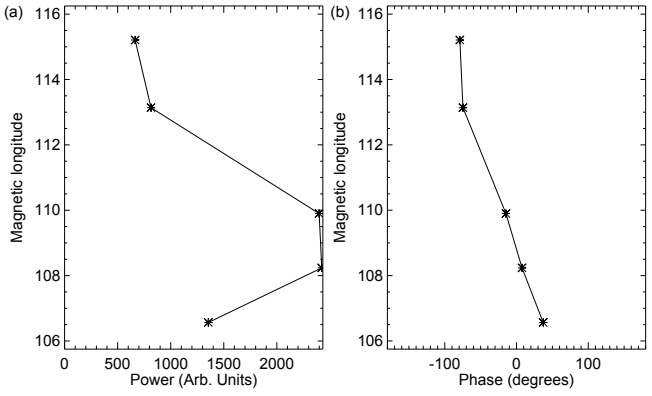

Fig. 6. Fourier **(a)** power and **(b)** phase at the peak frequency of the ULF wave observed in the ionospheric drift velocity measured along beams 7–12 of the Hankasalmi SuperDARN radar at 70° magnetic latitude as a function of geomagnetic longitude.

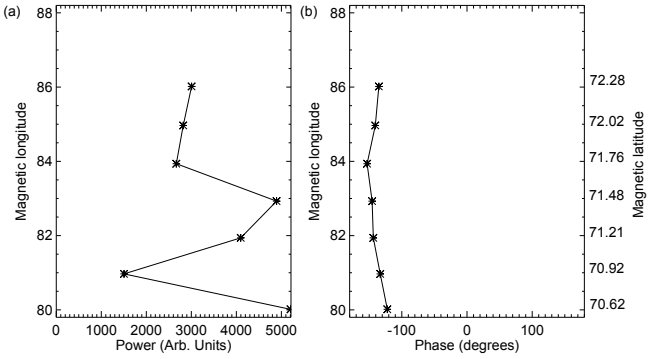

Fig. 7. Fourier **(a)** power and **(b)** phase at the peak frequency of the ULF wave observed in the ionospheric drift velocity measured along beam 5 of the Þykkvibær SuperDARN radar as a function of geomagnetic longitude. The corresponding geomagnetic latitudes of the datapoints are shown on the right for reference.

following substorm injection, with a drift resonance mechanism invoked as a source mechanism.

Following Yeoman and Wright (2001), taking the angular drift frequency of the particles to be

$$\omega_{\mathrm{d}} = \frac{\omega_{\mathrm{wave}}}{m_{\mathrm{wave}}} = \frac{2\pi}{\tau_{\mathrm{wave}} m_{\mathrm{wave}}}, \tag{3}$$

where τ_{wave} is the wave period (i.e. taking N=0 in Eq. 2) yields a proton angular drift frequency of $\sim 8.3\times10^{-4}$ rads s^{-1}. The wave observations presented here cover L-shells of 7.5–15. Applying the equations for the dependence of proton or electron drift on particle energy as in Yeoman and Wright (2001) then implies an energy source in 25–70 keV particles at L=7.5–15. Taking large pitch angles and the central L-shell of the wave observations, then particle energies of 33 keV are predicted. The characteristics of the ULF wave events with equatorward phase propagation observed by Grant et al. (1992), Yeoman et al. (1992), Yeoman and Wright (2001), Yeoman et al. (2008) and those presented here are summarised in Table 1, along with the energetic particle populations implicated in their generation by the authors concerned. Table 1 shows that whilst wave events are seen with a variety of m-numbers and periods, a clear trend exists in previous observations in that the energy of the proposed particle population inversion decreases as the L-shell of the observation increases.

The present observations lie outside this trend, being observed with relatively low m-numbers at relatively high latitudes. It is also the only observation with eastwards phase propagation. The present case study was taken from a larger database of such wave observations. The periods and m-numbers of the larger population were in fact very consistent. The majority of events identified so far have eastward phase propagation, although westward-propagating events have also been observed. Invoking the drift resonance mechanism for an eastward-propagating wave event clearly requires the wave energy source to lie in the population of energetic electrons rather than the population of energetic protons. Free energy should be available on occasion in the electron populations when the conditions in equations Eq. (1) and Eq. (2) are met for electrons, although in the case of electrons the much more rapid electron bounce period would preclude solutions for conditions other than $N = 0$ in Eq. (2). Such energy sources in drifting electron clouds have been considered as wave sources by Saka et al. (1992), Saka et al. (1996), Pilipenko et al. (2001a) and Pilipenko et al. (2001b). Such a mechanism involving electron clouds offers no explanation for the observed equatorward phase propagation, however. An alternative approach is considered below.

As is well known, in the $m \sim 1$ limit two MHD modes, the fast mode and the Alfvén, are coupled. However, when these two modes have a different parallel structure (Leonovich, 2001) this coupling may under some circumstances be neglected and the excitation of the Alfvén waves can be studied alone. The theory of the generation of this mode by substorm injected particles has been elaborated by Mager and Klimushkin (2008) and Mager et al. (2009). Although that theory was developed for the proton-driven high-m wave case, its qualitative features can be generalized for a more general situation, with lower m-numbers and a wave source in the energetic electron population (see Zolotukhina et al., 2008).

The azimuthally drifting inhomogeneity provided by the drifting cloud of injected energetic particles can be considered as a sudden impulse propagating from one location on the azimuthal coordinate to another with the drift angular velocity $\omega_{\mathrm{d}}(x)$. Thus, let us consider the Alfvén waves excited by a sudden impulse with an azimuthal structure of the form $e^{im\varphi}$, where m is the azimuthal wave number and φ is the azimuthal angle. Since the Alfvén waves represent field line oscillations, each field line having its own eigenfrequency (Hasegawa et al., 1983), the wave electric field is given by

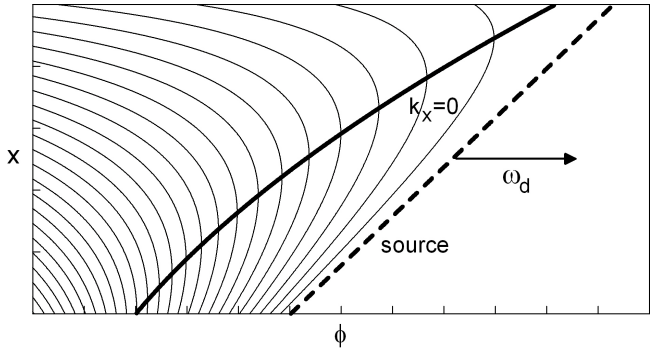

Fig. 8. Lines of constant modelled wave phase. The dashed line represents the drifting source (energetic particle cloud), positive ϕ is in the direction of the drift (westward for protons, eastward for electrons). The bold line corresponds to $k_x = 0$ (a purely poloidal polarization of the wave).

the expression (Leonovich and Mazur, 1998; Klimushkin and Mager, 2004)

$$E = |E|e^{i\Psi} \tag{4}$$

with the phase

$$\Psi = -\omega(x)t + m\varphi, \tag{5}$$

where ω is the resonant eigenfrequency and x is the radial coordinate. The azimuthal wave number m is determined by the exciting impulse.

Following Mager et al. (2009), for a wave source in an azimuthally drifting inhomogeneity, the expression for the wave field must show the fact that the Alfvén waves have negligible energy propagation transverse to field lines. Hence, Eq. (4) is replaced by

$$E = \Theta(\omega_{\rm d}t - \varphi)|E|e^{i\Psi}. \tag{6}$$

Here $\Theta(\omega_{\rm d}t - \varphi)$ is the Heaviside step function. The wave phase is still given by Eq. (5), but the m number is not arbitrarily imposed. Instead, as the excitation is due to a moving source, in the source reference system the (Doppler-shifted) phase just behind the source is constant, thus the transformed wave frequency $\omega' = \omega - m\omega_{\rm d}$ must be zero. Hence, we obtain an expression for the m-number:

$$m = \frac{\omega(x)}{\omega_{\rm d}(x)}, \tag{7}$$

just as in Eq. (3). This value depends on the radial coordinate (simply through the fact that different azimuthal wavenumbers will be resonant with the moving source at different L-shells). Finally, we get the following expression for the phase:

$$\Psi = -\omega(x)t + \frac{\omega(x)}{\omega_{\rm d}(x)}\varphi. \tag{8}$$

The bounce-averaged drift frequency in the inhomogeneous field is proportional to the particle energy ϵ and the radial coordinate x:

$$\omega_{\rm d} \simeq 8 \times 10^{-3}\epsilon x, \tag{9}$$

where $\omega_{\rm d}$, x, and ϵ are measured in degrees per minute, Earth radii, and keV, respectively (Roederer, 1970). The energy of substorm injected particles also depends on the radial coordinate, so in effect the drift frequency happens to depend only on the L-shell. Let us assume that drift frequency increases with the radial coordinate. This case can be realized in the magnetosphere under conditions where there is a considerable loss of injected protons (e.g. Southwood, 1980). In this case, the lines of constant phase in the x-φ plane are depicted in Fig. 8 (note that the whole picture is shifting to the right along with the source).

The wavevector radial component is determined as

$$k_x \equiv \Psi' = -\left(\frac{\omega}{\omega_{\rm d}}\right)'(\omega_{\rm d}t - \varphi) - \omega t\frac{\omega_{\rm d}'}{\omega_{\rm d}}, \tag{10}$$

where a prime indicates a radial derivative. Note that $\omega_{\rm d}t - \varphi \geq 0$ since the wave appears in some azimuthal location simultaneously with the particle cloud arrival in the same spot. Thus, provided that $\omega_{\rm d}' > 0$, the first right-hand side term is positive, while the second is negative. Just after the moment of the source passing a point with a given azimuthal coordinate, the radial component is negative, $k_x < 0$. However, it is finite, hence the wave has a polarization between toroidal and poloidal. A negative value of the wavevector radial component means a negative radial phase velocity of the wave; projected onto the ionosphere along geomagnetic field lines, this implies an equatorward phase propagation.

At the moment

$$t = \varphi\frac{(\omega/\omega_{\rm d})'}{\omega'} \tag{11}$$

k_x goes to zero the wave becomes poloidal. After that it changes its sign and becomes positive: the polarization of the wave becomes mixed again and, due to the phase mixing, the wave gradually transforms into toroidally-polarized one. The characteristic transformation time is

$$\tau = 2\frac{m_0 l}{\Omega_0 L}, \tag{12}$$

where m_0 and Ω_0 are a characteristic azimuthal wave number and angular frequency for the wave, L is the L-shell of the wave and l is a characteristic (magnetospheric) scale size (Mager and Klimushkin, 2008). If the wave attenuation is taken into account, then the wave does not have enough time to transform into a toroidal polarization, and the maximum wave amplitude will correspond to a mixed polarization with a pronounced poloidal component.

Table 1. A summary of the characteristics of this case study and previous ULF wave observations showing equatorward phase propagation, and the particle energy of their proposed magnetospheric source (after Yeoman et al., 2008).

Study	m	t (s)	L-shell	Implied particle energy (keV)
This study	+13	580	7.5–15	33
Yeoman et al. (2008)	−60	300	15	10
Grant et al. (1992)	∼ −50	∼300	7.5	20
Yeoman and Wright (2001)	−35	260	6.4	50
Yeoman et al. (1992)	∼ −20	∼400	5	60

5 Conclusion and discussion

The SuperDARN data presented in Sect. 3 showed that in the immediate aftermath of a substorm expansion phase onset, Pc5 Alfvén ULF wave activity was stimulated by the recently-injected energetic particles. Observations from the Hankasalmi radar revealed that the wave generated in the magnetosphere had a period of 580 s (a frequency of 1.7 mHz) and was characterized by an intermediate azimuthal wave number ($m = 13$), with an eastwards phase propagation. It had a significant poloidal component and a rapid equatorward phase propagation ($\sim 62^\circ$ per degree of latitude). The total equatorward phase variation over the wave signatures visible in the radar field-of-view exceeded the 180° associated with field line resonances. Data from a north-east directed beam of the Þykkvibær radar was consistent with the period and phase behaviour inferred from Hankasalmi. The wave period observed here was somewhat longer than previous observations of equatorward-propagating events (see Table 1). This may well be a consequence of the wave occurring very shortly after the substorm expansion, on stretched, near-midnight field lines characterised by longer eigenfrequencies than those involved in previous observations.

The data can be interpreted in terms of the theory of the wave generation by substorm injected particles as elaborated by Mager and Klimushkin (2008), Mager et al. (2009) and Zolotukhina et al. (2008), with, in this case an electron cloud of energy ∼33 keV acting as the wave source. According to the theory, wave comes into being with mixed polarization. As the wave moves farther and farther away from the source, it becomes poloidally-polarized. Furthermore, the wave finally transforms into a toroidal polarization. If the wave attenuation is taken into account (for example, due to the finite conductivity of the ionosphere or wave-particle interaction), then the wave does not have enough time to transform into a toroidal polarization, and the maximum wave amplitude will correspond to a mixed polarization. The azimuthal wave number m is determined by the wave eigenfrequency ω and the drift velocity of the source ω_d: $m \sim \omega/\omega_d$. Thus, to create the intermediate-m waves, the injected particles must have rather high energies for a given L-shell, in comparison to previous observations of wave events with equatorward polarization (see Table 1). The high energy and hence rapid azimuthal drift of the particles also explains the small time lag between the substorm onset and the detection of the wave.

Low and intermediate-m waves could also be generated by means of bump on tail instability under the drift resonance condition as outlined in Eq. (1) and Eq. (2) (Mager and Klimushkin, 2005). However, in this case there is a problem with the poloidal polarization of the wave, since the wave soon transforms into a toroidal one due to the phase mixing (Klimushkin, 2000, 2007; Klimushkin and Mager, 2004). In addition, this mechanism offers no explanation of the equatorward propagation of the wave. Besides, it would be more appropriate to regard the instability as a mechanism for wave enhancement rather than as the source. To set this mechanism to work requires some germ amplitude, which could be provided by the moving particle cloud source, as suggested in this paper. A statistical investigation into the characteristics of the new wave type presented here, and its relationship to the associated substorm activity, will be presented in a following paper.

Acknowledgements. This work is supported by INTAS grant 05-1000008-7978. The work by D.K. and P.M. is supported by Program of the presidium of the Russian Academy of Sciences #4, OFN RAS #15, and program #9 of the Earth's sciences department of the Russian academy of sciences. The work by T.K.Y. is supported by STFC grant ST/H002480/1. We thank Harald Frey for making the IMAGE substorm list publically available.

Topical Editor I. A. Daglis thanks W. J. Hughes and another anonymous referee for their help in evaluating this paper.

References

Agapitov, O., Glassmeier, K.-H., Plaschke, F., Auster, H.-U., Constantinescu, D., Angelopoulos, V., Magnes, W., Nakamura, R., Carlson, C. W., Frey, S., and McFadden, J. P.: Surface waves and field line resonances: A THEMIS case study, J. Geophys. Res., 114, A00C27, doi:10.1029/2008JA013553, 2009.

Allan, W., Poulter, E. M., and Nielsen, E.: STARE observations of a Pc5 pulsation with large azimuthal wave number, J. Geophys. Res., 87, 6163–6172, 1982.

Allan, W., Poulter, E. M., and Nielsen, E.: Pc5 pulsations associated with ring current proton drifts: STARE radar observations, Planet. Space Sci., 31, 1279–1289, 1983.

Anderson, B. J., Engebretson, M. J., Rounds, S. P., Zanetti, L. J., and Potemra, T. A.: A statistical study of Pc 3-5 pulsations observed by the AMPTE/CCE magnetic fields experiment. 1. Occurrence distributions, J. Geophys. Res., 95, 10495–10523, 1990.

Baddeley, L. J., Yeoman, T. K., and Wright, D. M.: HF doppler sounder measurements of the ionospheric signatures of small scale ULF waves, Ann. Geophys., 23, 1807–1820, doi:10.5194/angeo-23-1807-2005, 2005a.

Baddeley, L. J., Yeoman, T. K., Wright, D. M., Trattner, K. J., and Kellet, B. J.: On the coupling between unstable magnetospheric particle populations and resonant high *m* ULF wave signatures in the ionosphere, Ann. Geophys., 23, 567–577, doi:10.5194/angeo-23-567-2005, 2005b.

Chisham, G. and Orr, D.: Statistical studies of giant pulsations (Pgs): harmonic mode, Planet. Space Sci., 39, 999–1006, 1991.

Chisham, G., Lester, M., Milan, S. E., Freeman, M. P., Bristow, W. A., Grocott, A., McWilliams, K. A., Ruohoniemi, J. M., Yeoman, T. K., Dyson, P. L., Greenwald, R. A., Kikuchi, T., Pinnock, M., Rash, J. P. S., Sato, N., Sofko, G. J., Villain, J.-P., and Walker, A. D. M.: A decade of the Super Dual Auroral Radar Network (SuperDARN): scientific achievements, new techniques and future directions, Surv. Geophys., 28, 33–109, 2007.

Cowley, S. W. H. and Ashour-Abdallah, M.: Adiabatic plasma convection in a dipole field: Proton forbidden-zone effects for a simple electric field model, Planet. Space Sci., 24, 821–833, 1976.

Engebretson, M. J., Murr, D. L., Erickson, K. N., Strangeway, R. J., Klumpar, D. M., Fuselier, S. A., Zanetti, L. J., and Potemra, T. A.: The spatial extent of radial magnetic pulsation events observed in the dayside near synchronous orbit, J. Geophys. Res., 97, 13741–13758, 1992.

Eriksson, P. T. I., Blomberg, L. G., and Glassmeier, K.-H.: Cluster satellite observations of mHz pulsations in the dayside magnetosphere, Adv. Space Res., 38, 1730–1737, 2006.

Frey, H. U., Mende, S. B., Angelopoulos, V., and Donovan, E. F.: Substorm onset observations by IMAGE-FUV, J. Geophys. Res., 109, A10304, doi:10.1029/2004JA010607, 2004.

Glassmeier, K.-H., Buchert, S., Motschmann, U., Korth, A., and Pedersen, A.: Concerning the generation of geomagnetic giant pulsations by drift-bounce resonance ring current instabilities, Ann. Geophys., 17, 338–350, doi:10.1007/s00585-999-0338-4, 1999a.

Glassmeier, K.-H., Othmer, C., Cramm, R., Stellmacher, M., and Engebretson, M.: Magnetospheric field line resonance: a comparative approach, Surv. Geophys., 20, 61–109, 1999b.

Grant, I. F., McDiarmid, D. R., and McNamara, A. G.: A class of high-m pulsations and its auroral radar signature, J. Geophys. Res., 97, 8439–8451, 1992.

Greenwald, R. A., Weiss, W., Nielsen, E., and Thomson, N. P.: STARE: A new radar auroral backscatter experiment in northern Scandinavia, Radio Sci., 13, 1021–1039, 1978.

Greenwald, R. A., Baker, K. B., Dudeney, J. R., Pinnock, M., Jones, T. B., Thomas, E. C., Villain, J.-P., Cerisier, J.-C., Senior, C., Hanuise, C., Hunsucker, R. D., Sofko, G., Koehler, J., Nielsen, E., Pellinen, R., Walker, A. D. M., Sato, N., and Yamagishi, H.: DARN/SUPERDARN A global view of the dynamics of high-latitude convection, Space Sci. Rev., 71, 761–796, 1995.

Hasegawa, A., Tsui, K. N., and Assis, A. S.: A theory of long period magnetic pulsations. 3. Local field line oscillations, Geophys. Res. Lett., 10, 765–767, 1983.

Hughes, W. J., Southwood, D. J., Mauk, B., McPherron, R. L., and Barfield, J. N.: Alfvén waves generated by an inverted plasma energy distribution, Nature, 275, 43–45, 1978.

Hughes, W. J., McPherron, R. L., Barfield, J. N., and Mauk, B. H.: A compressional Pc4 pulsation observed by three satellites in geostationary orbit near local midnight, Planet. Space Sci., 27, 821–840, 1979.

Klimushkin, D. Y.: The propagation of high-*m* Alfvén waves in the Earth's magnetosphere and their interaction with high-energy particles, J. Geophys. Res., 105, 23303–23310, 2000.

Klimushkin, D. Y.: How energetic particles construct and destroy poloidal high-*m* Alfvén waves in the magnetosphere, Planet. Space Sci., 55, 722–730, 2007.

Klimushkin, D. Yu. and Mager, P. N.: The spatio-temporal structure of impulse-generated azimuthalsmall-scale Alfvén waves interacting with high-energy chargedparticles in the magnetosphere, Ann. Geophys., 22, 1053–1060, doi:10.5194/angeo-22-1053-2004, 2004.

Kokubun, S.: Statistical characteristics of Pc5 waves at geostationary orbit, J. Geomag. Geoelectr., 37, 759–779, 1985.

Leonovich, A. S.: A theory of field line resonance in a dipole-like axisymmetric magnetosphere, J. Geophys. Res., 106(A11), 25803–25812, doi:10.1029/2001JA000104, 2001.

Leonovich, A. S. and Mazur, V. A.: Standing Alfvén waves with $m \gg 1$ in an axisymmetric magnetosphere excited by a non-stationary source, Ann. Geophys., 16, 914–920, doi:10.1007/s00585-998-0914-z, 1998.

Lessard, M. R., Hudson, M. K., and Lühr, H.: A statistical study of Pc 3-Pc 5 magnetic pulsations observed by the AMPTE/Ion Release Module satellite, J. Geophys. Res., 104, 4523–4538, 1999.

Lühr, H.: The IMAGE magnetometer network, STEP International Newsletter, 4, 4–6, 1994.

Mager, P. N. and Klimushkin, D. Yu.: Spatial localization and azimuthal wave numbers of Alfvén waves generated by drift-bounce resonance in the magnetosphere, Ann. Geophys., 23, 3775–3784, doi:10.5194/angeo-23-3775-2005, 2005.

Mager, P. N. and Klimushkin, D. Yu.: Alfvén ship waves: high-*m* ULF pulsations in the magnetosphere generated by a moving plasma inhomogeneity, Ann. Geophys., 26, 1653–1663, doi:10.5194/angeo-26-1653-2008, 2008.

Mager, P. N., Klimushkin, D. Y., and Ivchenko, N.: On the equatorward phase propagation of high-m ULF pulsations observed by radars, J. Atmos. Solar-Terr. Phys., 71, 1677–1680, doi: 10.1016/j.jastp.2008.09.001, 2009.

McNamara, A. G., McDiarmid, D. R., Sofko, G. J., Koeler, J. A., Forsyth, P. A., and Moorcroft, D. R.: BARS – a dual bistatic auroral radar system for the study of electric fields in the Canadian sector of the auroral zone, Adv. Space Res., 2, 145–148, 1983.

Mende, S. B., Heetderks, H., Frey, H. U., Lampton, M., Geller, S. P., Abiad, R., Siegmund, O. H. W., Tremsin, A. S., Spann, J., Dougani, H., Fuselier, S. A., Magoncelli, A. L., Bumala, M. B., Murphree, S., and Trondsen, T.: Far ultraviolet imaging from the IMAGE spacecraft. 2. Wideband FUV imaging, Space Sci. Rev., 91, 271–285, 2000a.

Mende, S. B., Heetderks, H., Frey, H. U., Lampton, M., Geller, S. P., Habraken, S., Renotte, E., Jamar, C., Rochus, P., Spann, J.,

Fuselier, S. A., Gerard, J.-C., Gladstone, R., Murphree, S., and Cogger, L.: Far ultraviolet imaging from the IMAGE spacecraft. 1. System design, Space Sci. Rev., 91, 243–270, 2000b.

Nielsen, E., Guttler, W., Thomas, E. C., Stewart, C. P., Jones, T. B., and Hedburg, A.: SABRE – new radar-auroral backscatter experiment, Nature, 304, 712–714, 1983.

Ozeke, L. G. and Mann, I. R.: Modeling the properties of high *m* Alfvén waves driven by the drift-bounce resonance mechanism, J. Geophys. Res., 106, 15583–15597, 2001.

Pilipenko, V., Kleimenova, N., Kozyreva, O., Engebretson, M., and Rasmussen, O.: Long-period magnetic activity during the May 15, 1997 storm, J. Atmos. Solar-Terr. Phys., 63, 489–501, 2001a.

Pilipenko, V. A., Watermann, J., Popov, V. A., and Papitashvili, V. O.: Relationship between auroral electrojet and Pc5 ULF waves, J. Atmos. Sol.-Terr. Phys., 63, 1545–1557, 2001b.

Roederer, J. G.: Dynamics of geomagnetically trapped radiation, Springer-Verlag, Berlin, Heidelberg, New York, 1970.

Saka, O., Iijima, T., Yamagishi, H., Sato, N., and Baker, D. N.: Excitation of Pc 5 pulsations in the morning sector by a local injection of particles in the magnetosphere, J. Geophys. Res., 97, 10693–10701, 1992.

Saka, O., Watanabe, O., and Baker, D. N.: A possible driving source for transient field line oscillations in the postmidnight sector at geosynchronous altitudes, J. Geophys. Res., 101, 24719–24726, 1996.

Schäfer, S., Glassmeier, K. H., Eriksson, P. T. I., Pierrard, V., Fornaçon, K. H., and Blomberg, L. G.: Spatial and temporal characteristics of poloidal waves in the terrestrial plasmasphere: a CLUSTER case study, Ann. Geophys., 25, 1011–1024, doi:10.5194/angeo-25-1011-2007, 2007.

Schäfer, S., Glassmeier, K. H., Eriksson, P. T. I., Mager, P. N., Pierrard, V., Fornaçon, K. H., and Blomberg, L. G.: Spatio-temporal structure of a poloidal Alfvén wave detected by Cluster adjacent to the dayside plasmapause, Ann. Geophys., 26, 1805–1817, doi:10.5194/angeo-26-1805-2008, 2008.

Southwood, D. J.: A general approach to low-frequency instability in the ring current plasma, J. Geophys. Res., 81, 3340–3348, 1976.

Southwood, D. J.: Low frequency pulsation generation by energetic particles, J. Geomagn. Geoelectr., Suppl. II, 32, 75–88, 1980.

Southwood, D. J., Dungey, J. W., and Etherington, R. J.: Bounce resonant interactions between pulsations and trapped particles, Planet. Space Sci., 17, 349–361, 1969.

Takahashi, K., Higbie, P. R., and Baker, D. N.: Azimuthal propagation and frequency characteristic of compressional Pc5 waves observed at geostationary orbit, J. Geophys. Res., 90, 1473–1485, 1985.

Takahashi, K., McEntire, R. W., Lui, A. T. Y., and Potemra, T. A.: Ion flux oscillations associated with a radially polarised transverse Pc5 magnetic pulsation, J. Geophys. Res., 95, 3717–3731, 1990.

Takahashi, K., Sato, N., Warnecke, J., Lühr, H., Spence, H. E., and Tonegawa, Y.: On the standing wave mode of giant pulsations, J. Geophys. Res., 97, 10717–10732, 1992.

Tian, M., Yeoman, T. K., Lester, M., and Jones, T. B.: Statistics of Pc5 pulsation events observed by SABRE, Planet. Space Sci., 39, 1239–1247, 1991.

Waldock, J. A., Jones, T. B., and Southwood, D. J.: First results of micropulsation activity observed by SABRE, Planet. Space Sci., 31, 573–578, 1983.

Woch, J., Kremser, G., and Korth, A.: A comprehensive investigation of compressional ULF waves observed in the ring current, J. Geophys. Res., 95, 15113–15132, 1990.

Wright, D. M., Yeoman, T. K., and Chapman, P. J.: High-latitude HF Doppler observations of ULF waves. 1. Waves with large spatial scale sizes, Ann. Geophys., 15, 1548–1556, doi:10.1007/s00585-997-1548-2, 1997.

Yeoman, T. K. and Wright, D. M.: ULF waves with drift resonance and drift-bounce resonance energy sources as observed in artificially-induced HF radar backscatter, Ann. Geophys., 19, 159–170, doi:10.5194/angeo-19-159-2001, 2001.

Yeoman, T. K., Tian, M., Lester, M., and Jones, T. B.: A study of Pc5 hydromagnetic waves with equatorward phase propagation, Planet. Space Sci., 40, 797–810, 1992.

Yeoman, T. K., Wright, D. M., Chapman, P. J., and Stockton-Chalk, A. B.: High-latitude observations of ULF waves with large azimuthal wavenumbers, J. Geophys. Res., 105, 5453–5462, 2000.

Yeoman, T. K., Baddeley, L. J., Dhillon, R. S., Robinson, T. R., and Wright, D. M.: Bistatic observations of large and small scale ULF waves in SPEAR-induced HF coherent backscatter, Ann. Geophys., 26, 2253–2263, doi:10.5194/angeo-26-2253-2008, 2008.

Zolotukhina, N. A., Mager, P. N., and Klimushkin, D. Yu.: Pc5 waves generated by substorm injection: a case study, Ann. Geophys., 26, 2053–2059, doi:10.5194/angeo-26-2053-2008, 2008.